



Design and implementation of a modified DC-DC converter suitable for renewable energy application

Tareq ALNEJAILI and Said DRID senior member IEEE

Laboratory, LSP-IE, University of Batna, Rue Chahid M^{ed} El-Hadi Boukhlof BATNA 05000, ALGERIE

Maystro1988@outlook.com, saiddrid@ieee.org

Abstract-- This paper presents a novel design, simulation and realization of modified buck, boost and buck-boost converter with wide range of output voltage suitable for MPPT charge controller for different solar batteries or other applications. This system has a nonlinear dynamic behavior, as it works in switch-mode.

In this paper we analyze the equations of all modes, discuss new simple control circuit and example shows the application of this converter in solar battery charger.

Key words-- maximum power point tracking (MPPT), Dc-DC converter, solar battery.

1. Introduction

DC- DC converters play an important role in renewable energy applications and other applications, the input of these converters is an unregulated DC voltage, which is obtained by PV array. Figure (1), shows the schematic circuit of the modified converter it can convert the supply voltage much higher, much lower and around it value while leaving voltage polarity unchanged.

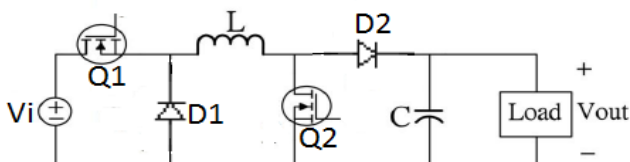


Fig.1 Schematic circuit of the modified converter

Table (1) Summarizes the operation of the modified converter, this converter can be used as a buck converter or as a boost converter or as a buck-boost converter by selecting different combinations of switches Q1 and Q2 driven by the PWM1 and PWM2 signals output by the microcontroller. [1] The next sections will discuss new simple control circuit and example shows the application of this converter in solar battery charger.

Tab.1 Operation of the modified converter

Converter mode	Q1	Q2	Average load voltage
Boost	Always ON	Inductor charge: ON Inductor discharge: OFF	$V_o = \frac{V_i}{1-D}$
Buck	Inductor charge: ON Inductor discharge: OFF	Always OFF	$V_o = D V_i$
Buck-boost	Inductor charge: ON Inductor discharge: OFF	Inductor charge: ON Inductor discharge: OFF	$V_o = \frac{D V_i}{1-D}$

Where: V_i is the input voltage

V_o is the output voltage

D is the duty cycle of the converter



**Le 3^{ème} Séminaire International sur les Energies Nouvelles et
Renouvelables**

**The 3rd International Seminar on New and Renewable
Energies**

Unité de Recherche Appliquée en Energies Renouvelables,

Ghardaïa – Algérie 13 et 14 Octobre 2014



2. Principal of operation

The power generated from the PV panel is variable during the days due to the change in irradiance and temperature, the input voltage of the converter is restricted to the PV panel output voltage range of 10V to 35V, the minimum required voltage for control system is 9V. The converter can provide wide range of output voltage under the input range voltage, when the required voltage is much higher than the input voltage the converter works as boost converter by keeping Q1 always in ON condition and drive Q2, so keeping Q1 always in ON condition require 100% PWM1 duty cycle ,practically PWM duty cycle can't go for 100% and even it can go for that limit, this will reduce the service life of the semiconductor component, simple solution will be discussed here .Figure(2) shows that a relay is place in series with the switch Q1 when the boost mode is desired the microcontroller will send signal and the relay will change its condition and the converter will work in boost mode ,by driving the switch Q2. So as we have seen with this solution we can increase the service life of the component and get the desire mode. When the required voltage is much smaller than the input voltage the converter will work in buck mode by keeping Q2 in OFF condition, this can be done by using simple switch controlled by the microcontroller. Finally when the required voltage is around the input voltage the converter will work in buck-boost mode by driving Q1 and Q2 (PWM1=PWM2 same frequency and same duty cycle).

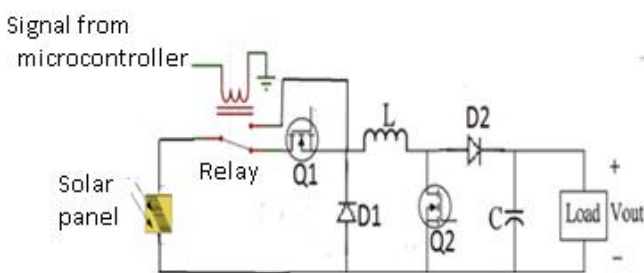


Fig.2 Boost mode solution

3. DC Analysis of PWM modified Converter for CCM

The switch Q1, Q2 is controlled by a pulse-width modulator and is turned on and off at the switching frequency $f_s = 1/T$, the duty cycle D defined as $D = t_{on}/T$.

3.1 Buck mode

As we mention before the switch Q2 always in OFF condition, and we drive the switch Q1, table (2) Summarizes the DC analyze for this mode:

Tab.2 DC analyze for buck mode

Time interval	Switch Q1,diode D1	Inductor current, and ripple inductor current	Inductor voltage
$0 < t \leq DT$	Q1 is ON, D1 is OFF	$i_L = \frac{V_i - V_o}{L}t + I_L(0)$ $\Delta i_L = \frac{(V_i - V_o)D}{f_s L}$	$v_L = V_i - V_o = L \frac{di_L}{dt}$
$DT < t \leq T$	Q1 is OFF, D1 is ON	$i_L = \frac{-V_o}{L}(t - DT) + I_L(DT)$ $\Delta i_L = \frac{(1 - D)V_o}{f_s L}$	$v_L = -V_o = L \frac{di_L}{dt}$

3.2 Boost mode

The switch Q1 always in ON condition and we drive the switch Q2, table (3) Summarizes the DC analyze for this mode.

Tab.3 DC analyze for boost mode

Time interval	Switch Q2,diode D2	Inductor current, and ripple inductor current	Inductor voltage
$0 < t \leq DT$	Q2 is ON, D2 is OFF	$i_L = \frac{V_i}{L}t + I_L(0)$ $\Delta i_L = \frac{D(1 - D)V_o}{f_s L}$	$v_L = V_i = L \frac{di_L}{dt}$
$DT < t \leq T$	Q2 is OFF, D2 is ON	$i_L = \frac{V_i - V_o}{L}(t - DT) + I_L(DT)$ $\Delta i_L = \frac{D(1 - D)V_o}{f_s L}$	$v_L = V_i - V_o = L \frac{di_L}{dt} < 0$

3.3 Buck-boost

By driving Q1 and Q2 with tow signals equal in frequency and in the duty cycle, the converter works in buck-boost mode, table (4) Summarizes the DC analyze for this mode:



Le 3^{ème} Séminaire International sur les Energies Nouvelles et Renouvelables

The 3rd International Seminar on New and Renewable Energies

Unité de Recherche Appliquée en Energies Renouvelables,

Ghardaïa – Algérie 13 et 14 Octobre 2014



Table (4): DC analyze for buck-boost mode.

Time interval	Switch Q1,Q2, diodeD2,D2	Inductor current, and ripple inductor current	Inductor voltage
$0 < t \leq DT$	Q1 and Q1 is ON, D1 and 2 is OFF	$i_L = \frac{V_i}{L}t + I_L(0)$ $\Delta i_L = \frac{(1-D)V_o}{f_s L}$	$v_L = V_i$ $= L \frac{di_L}{dt}$
$DT < t \leq T$	Q1 and Q1 is OFF, D1 and 2 is ON	$i_L = \frac{-V_o}{L}(t - DT) + i_L(DT)$ $\Delta i_L = \frac{(1-D)V_o}{f_s L}$	$v_L = -V_o$ $= L \frac{di_L}{dt}$

4. Application of this converter in solar battery charger

As one of the important application of the converter ,solar battery charger for different solar batteries (48V, 24V, 12V) , Initially the converter works in Buck-Boost converter mode charging the battery with constant voltage, as soon as there is an overflow condition for the duty cycle(the input voltage much smaller than the desired output voltage). The converter switches from buck-boost converter mode to boost converter mode. The microcontroller program has 3 routine the first for 12V lead acid battery, the second for 24 lead acid batteries, and the third for 48lead acid battery.

For example if we want to charge 48V solar battery, as soon as we connect the battery, the microcontroller will measure it voltage so the program will enter the third routine and it will keep measuring the input voltage, if the input voltage is much smaller than the battery voltage, then The converter switches from buck-boost converter mode to boost converter mode (the relay will change its initial condition and we will drive Q2), for assume the safety the design contain switch (relay)that is used to connect or disconnect the Load from the battery, depending on the terminal voltage of the battery and current drawn by the load, protection of the battery from deep charge and overload.

5. Design data for the converter

The specification of all converter modes is: input voltage 10V to 35V dc, output voltage for boost mode is 48.8V to 50.8V, output voltage for buck-boost mode is varying from 26V to 14V,maximum load current for all modes is 6.4A,

Allowable ripple voltage 5% of maximum output voltage and 10% of maximum average current. Switching frequency=100 KHz.

5.1. Selection of the inductor

A converter operates in continuous mode if the current through the inductor (I_L) never falls to zero during the commutation cycle, so combination of the inductor size and switching frequency must be carefully chosen when the inductor is sizing, large inductance values tend to increase the start-up time slightly, small inductance values allow the coil current to ramp up to higher levels before the switch turns off [2],and high switching frequency tend to increase the switching loss in the converter, table (5) summarizes the inductor calculation for all modes . The highest value will be chosen for the design to ensure that the converter operates in continuous mode.

Tab5. Inductor calculation for all modes

Convert er mode	Inductance Formula	Inductance calculation
Boost	$L = \frac{D(1-D)V_o}{f_s * \Delta i_L}$	$L == 1.08mH$
Buck-boost 24V	$L = \frac{(1-D)V_o}{f_s * \Delta i_L}$	$L == 1.37mH$
Buck-boost 12V	$L = \frac{(1-D)V_o}{f_s * \Delta i_L}$	$L == 0.85mH$

5.2. Selection of the capacitance required

The basic selection of the output capacitor is based on the ripple current and ripple voltage, the effective series resistance (ESR) of the output capacitor and the inductor value directly affect the output ripple voltage. Low-ESR capacitors will be used for best performance. For reducing ESR is also possible to connect few capacitors in parallel. An approximate calculation for the required output capacitance for all modes is summarized in table (6) [7].



**Le 3^{ème} Séminaire International sur les Energies Nouvelles et
Renouvelables**

**The 3rd International Seminar on New and Renewable
Energies**

Unité de Recherche Appliquée en Energies Renouvelables,

Ghardaïa – Algérie 13 et 14 Octobre 2014



Tabl.6 required output capacitance calculation

Converter mode	Capacitance formula	Capacitance calculation
Boost	$C_{min} = \frac{D_{max} * V_o * 2}{f_s * R_{lmin} * V_r}$	$C_{min} = 188.2\mu F$
Buck-boost 24V	$C_{min} = \frac{D_{max} * V_o * 2}{f_s * R_{lmin} * V_r}$	$C_{min} = 192.5\mu F$
Buck-boost 12V	$C_{min} = \frac{D_{max} * V_o * 2}{f_s * R_{lmin} * V_r}$	$C_{min} = 188.3\mu F$

Where: V_r : The output ripple voltage which equal the allowable ripple voltage Multiplied by the output voltage
 R_{lmin} : is the minimum load resistance match in this case the internal battery resistance.

The chosen value for the output capacitor is $220\mu F$.
There for the value of the input capacitor allowing having a ripple less than ΔV_{pv} must satisfy [3]:

$$C_i \Rightarrow \frac{I_{pvmax}}{f \cdot \Delta V_{pvmax}} = 146.6\mu F$$

Where I_{pvmax} : is maximum input current.
 ΔV_{pv} : is the PV ripple voltage

5.3. Selection of the diode and the semiconductor

Four parameters must be considered when selecting the diode for DC-DC converter application. First, the reverse breakdown voltage of the diode must be greater than the voltage at the output of the converter for the diode D2 and at the input voltage for the diode D1. Second, the diode must be able to operate with the forward current that will be pushed through the diode by the inductor. Third, to minimize power loss when the diode is conducting, the forward voltage should be as small as possible. Finally, choosing a diode with a short reverse-recovery time will limit the output charge lost back to the input when the diode switches from the conducting to the non conducting stage [4].

The transistor selected must be able to withstand the drain-to-source voltage that occurs when the inductor is discharging through the diode. The rated drain current of the transistor needs to be greater than the peak inductor current. To minimize switching losses, an optimal transistor will also have low gate-to-source and drain-to-source capacitances.

The maximum voltage and current stresses of the switch Q1 and the diode D1 in CCM for steady state operation is [7]

$$V_{sm1} = V_{DM1} = V_{imax} \quad (1)$$

$$I_{sm1} = I_{DM1} = I_o + \frac{\Delta i_L}{2} \\ = I_{omax} + \frac{(V_{imax} - V_o) D_{min}}{2 * f_s * L} \quad (2)$$

Where V_{sm1} and V_{DM1} are the voltage stresses of the switch Q1 and the diode D1 respectively.

I_{sm1} , I_{DM1} Are the current stresses of the switch Q1 and the diode D1 respectively.

The maximum voltage and current stresses of the switch Q2 and the diode D2 in CCM for steady state operation is [7]

$$V_{sm2} = V_{DM2} = V_{omax} \quad (3) \\ I_{sm2} = I_{DM2} = I_i + \frac{\Delta i_{Lmax}}{2} \\ = \frac{I_{omax}}{1 - D_{max}} + \frac{D(1 - D)V_o}{2 * f_s * l} \quad (4)$$

Where V_{sm2} and V_{DM2} are the voltage stresses of the switch Q2 and the diode D2 respectively.

I_{sm2} , I_{DM2} are the current stresses of the switch Q2 and the diode D2 respectively.

6. Stability analysis

Figure (3), shows Schematic circuit of the modified converter considering battery and PV models, the input is an unregulated DC voltage, which is obtained by PV array which has non linear characteristic because it output power is effected by changing in the irradiance and temperature, the converter uses to charge various solar batteries whose have non linear model too, so an analytical solution is needed which is very difficult to develop for such a nonlinear time-varying system. Under constant and uniform irradiance and cell temperature levels, the system operates around the MPP and it is possible to develop a linearized analytical model to characterize system behavior around this equilibrium point. so this can be done by small-signal analysis around the MPP point.

as we seen in the figure(3), the PV chosen model is THEVENIN model which is consist of voltage source, and a resistor R_m in series connection as the internal resistance, this model takes into account the PV open-circuit voltage, which depends on the PV temperature [5], then it allows to analyze thermal effects.



Simple battery model [6] is chosen too this model consists of only ideal battery V_b as the electromotive force of a battery, and a resistor R_s in series connection as the internal resistance.

$$\frac{dV_i}{dt} = \frac{V_{oc}}{R_m * C_i} - \frac{V_i}{R_m * C_i} - \frac{i_L}{C_i} \quad (6)$$

$$\frac{dV_s}{dt} = \frac{-V_s}{C_s * R_s} + \frac{V_b}{R_s * C_s} + \frac{(1-h)i_L}{C_s} \quad (7)$$

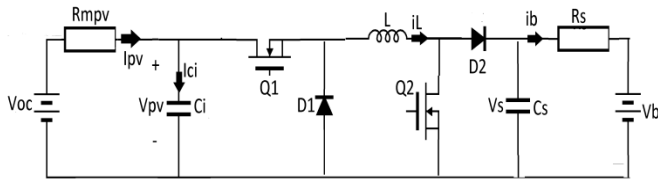


Fig.3 Schematic circuit of the modified converter considering battery and PV models

6.1. Stability analysis for boost mode

At this mode figure (4), the dynamic equations are defined to represent the system in state space, where the state variables are the inductor current, the input capacitor voltage and the output capacitor voltage, while the system inputs are the converter, temperature represented by the V_{oc} voltage, and the converter output voltage (the battery voltage).

This system is clearly non-linear, and present several configuration so first of all we will calculate the topology compact model, after we will pass by the average large signal model, after this step we will get a matrix which it continuously over a period but it still not linear finally to linearized the system we will applied the average small signal model.

In matrix form

$$\frac{d}{dt} \begin{bmatrix} i_L \\ V_i \\ V_s \end{bmatrix} = \begin{bmatrix} 0 & 1/L & h - 1/L \\ -1/C_i & -1/R_m * C_i & 0 \\ 1 - h/C_s & 0 & -1/C_s * R_s \end{bmatrix} \begin{bmatrix} i_L \\ V_i \\ V_s \end{bmatrix} + \begin{bmatrix} 0 & 0 \\ 1/R_m * C_i & 0 \\ 0 & 1/R_m * C_s \end{bmatrix} \begin{bmatrix} V_{oc} \\ V_b \end{bmatrix}$$

$$A_h = \begin{bmatrix} 0 & 1/L & h - 1/L \\ -1/C_i & -1/R_m * C_i & 0 \\ 1 - h/C_s & 0 & -1/C_s * R_s \end{bmatrix}$$

$$B_h = \begin{bmatrix} 1 & 0 \\ R_m * C_i & 0 \\ 0 & 1/R_m * C_s \end{bmatrix}$$

Where h is the switching function, $h \in [0, 1]$

The matrices A_h and B_h are discontinuous and non linear so on pass to the matrices A_α and B_α which they are continuous but they still non linear.

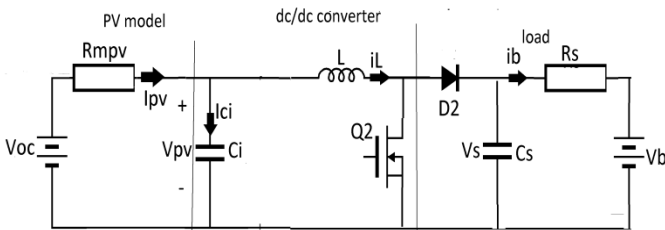


Fig.4 Schematic circuit of the modified converter considering battery and PV models (boost mode)

6.1.1. The topology compact model

After analysis of different operation period, the topology compact model be written as

$$\frac{di_L}{dt} = \frac{V_i}{L} - \frac{(1-h)V_s}{L} \quad (5)$$

$$A_\alpha = \begin{bmatrix} 0 & 1/L & \alpha - 1/L \\ -1/C_i & -1/R_m * C_i & 0 \\ 1 - \alpha/C_s & 0 & -1/C_s * R_s \end{bmatrix}$$

$$B_\alpha = \begin{bmatrix} 0 & 0 \\ 1 & 0 \\ R_m * C_i & 1/R_m * C_s \end{bmatrix}$$



Where α the duty cycle of the converter. We can extract the equation of state variable

$$\frac{di_L}{dt} = \frac{Vi}{L} - \frac{(1-\alpha)V_s}{L} \quad (8)$$

$$\frac{dvi}{dt} = \frac{Voc}{R_m * C_i} - \frac{Vi}{R_m * C_i} - \frac{i_L}{C_i} \quad (9)$$

$$\frac{dvs}{dt} = \frac{-V_s}{C_s * R_s} + \frac{V_b}{R_s * C_s} + \frac{(1-\alpha)i_L}{C_s} \quad (10)$$

Laplace transformation is applied in the previous equations

$$L * S * I_L = Vi - (1-\alpha)V_s \quad (11)$$

$$C_i * S * V_i = -I_L - \frac{Vi}{R_m} + \frac{Voc}{R_m} \quad (12)$$

$$C_s * S * V_s = (1-\alpha)I_L - \frac{V_s}{R_s} + \frac{V_b}{R_s} \quad (13)$$

6.1.3. The average small signal model

The model is linearized around the operating point, we consider only the change in the command, and the change in output voltage is neglected ($\Delta V_s = 0$) due to the presence of the battery at the converter output. After using of total differential law at the previous equations we obtained:

$$L * S * \Delta i_L = \Delta Vi - V_s \Delta \alpha \quad (14)$$

$$C_i * S * \Delta Vi = -\Delta i_L - \frac{1}{R_m} \Delta Vi \quad (15)$$

$$\Delta i_L = \frac{\Delta Vi - V_s \Delta \alpha}{LS} \quad (16)$$

$$C_i * \Delta Vi * S + \frac{\Delta Vi}{R_m} = - \left(\frac{\Delta Vi + V_s \Delta \alpha}{LS} \right) \gg$$

$$\Delta Vi \left(C_i * S + \frac{1}{R_m} + \frac{1}{L * S} \right) L * S = -V_s \Delta \alpha \quad (17)$$

So the array voltage to duty ratio small signal transfer function is given by

$$\frac{\Delta Vi}{\Delta \alpha} = \frac{-R_m * V_s}{R_m * L * C_i * S^2 + L * S + R_m} \quad (18)$$

The coefficients of the transfer function can be calculated by substituting the system parameter values given below. These parameters were obtained by a combination of measurement, and design choice,

$R_m=15.9\Omega$, $V_s=48V$, $L=1.5mH$, $C_i=150\mu F$.

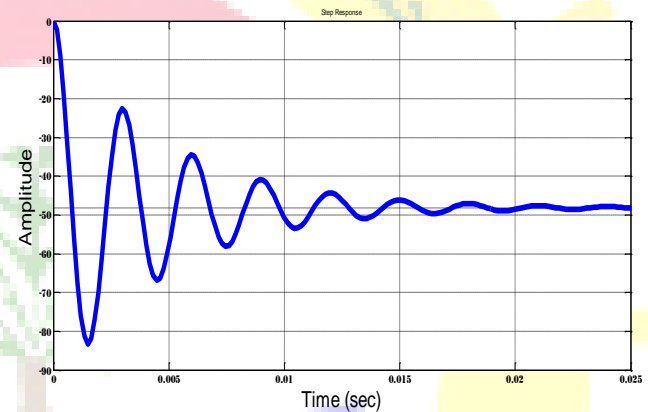


Fig.5 Array voltage response to a step increase in duty ratio.

This transfer function has two complex conjugate poles at $S=1.0e+003 * (-0.2101 \pm 2.0972i)$, the response for a step increase in duty ratio is illustrated in Fig (5).

The signal has a negative steady-state gain of about 48, the rise time is about 0.5 ms, the settling time is about 14 ms, the peak overshoot is about 73.5%, the natural frequency is 2108rad/S and the damping factor is 0.1.

6.2. Stability analysis for Buck-Boost mode

Figure (3) represents Schematic circuit of the buck converter considering battery and PV models



Le 3^{ème} Séminaire International sur les Energies Nouvelles et Renouvelables

The 3rd International Seminar on New and Renewable Energies

Unité de Recherche Appliquée en Energies Renouvelables,

Ghardaïa - Algérie 13 et 14 Octobre 2014



6.2.1. The average large signal model is:

$$A\alpha = \begin{bmatrix} 0 & \frac{\alpha}{L} & \alpha - \frac{1}{L} \\ -\frac{\alpha}{C_i} & -\frac{1}{R_m * C_i} & 0 \\ 1 - \frac{\alpha}{C_s} & 0 & -\frac{1}{C_s * R_s} \end{bmatrix}$$

$$B\alpha = \begin{bmatrix} 0 & 0 & 0 \\ \frac{1}{R_m * C_i} & 0 & 0 \\ 0 & \frac{1}{R_m * C_s} & 1 \end{bmatrix}$$

We can extract the equation of state Variable

$$\frac{di_L}{dt} = \frac{\alpha V_i}{L} - \frac{(1-\alpha)V_s}{L} \quad (19)$$

$$\frac{dV_i}{dt} = \frac{V_{oc}}{R_m * C_i} - \frac{V_i}{R_m * C_i} - \frac{\alpha i_L}{C_i} \quad (20)$$

$$\frac{dV_s}{dt} = \frac{-V_s}{C_s * R_s} + \frac{V_b}{R_s * C_s} + \frac{(1-\alpha)i_L}{C_s} \quad (21)$$

Laplace transformation is applied in the equations

$$L * S * I_L = \alpha V_i - (1-\alpha)V_s \quad (22)$$

$$C_i * S * V_i = -\alpha I_L - \frac{V_i}{R_m} + \frac{V_{oc}}{R_m} \quad (23)$$

$$C_s * S * V_s = (1-\alpha)I_L - \frac{V_s}{R_s} + \frac{V_b}{R_s} \quad (24)$$

6.2.2. The average small signal model

The model is linearized around the operating point, we consider only the change in the command, and the change in output voltage is neglected ($\Delta V_s = 0$). After using of total differential law at the previous equations we obtained:

$$L * S * \Delta i_L = \alpha \Delta V_i - V_i \Delta \alpha \quad (25)$$

$$C_i * S * \Delta V_i = -\alpha \Delta i_L - I_L \Delta \alpha - \Delta V_i \frac{1}{R_m} \quad (26)$$

$$\Delta i_L = \frac{\alpha \Delta V_i + V_i \Delta \alpha + V_s \Delta \alpha}{L * S} \quad (27)$$

After replaces the previous equations, the array voltage to duty ratio small signal transfer function is given by

$$\frac{\Delta V_i}{\Delta \alpha} = \frac{-L * I_L * S - \alpha (V_i + V_s)}{L * C_i * S^2 + \frac{L}{R_m} * S + \alpha^2} \quad (28)$$

Where $V_s=24V$, $\alpha = 0.428$, $I_L=5A$, $R_m=15.9\Omega$, $C_i=150F$, $L=1.5mH$ and $V_i=35V$.

This transfer function has two complex conjugate poles at $S=1.0e+002 * (-2.0889 \pm 8.7779i)$, the response for a step increase in duty ratio is illustrated in Fig (6).

The signal has a negative steady-state gain of about 140.3, the rise time is about 1.39 ms, the settling time is about 12 ms, the peak overshoot is about 46.8%, the natural frequency is 902rad/S and the damping factor is 0.23.

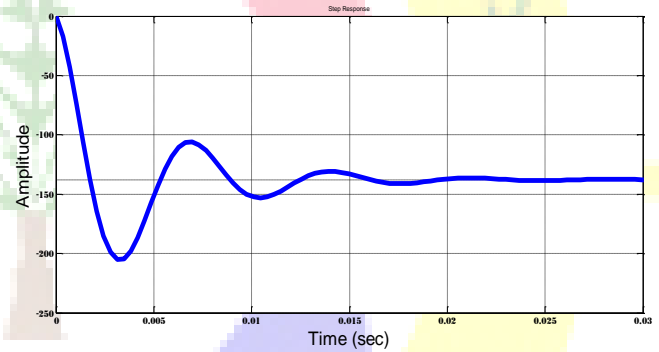


Fig.6 Array voltage response to a step increase in duty ratio.

Case of 12V battery

Where $V_s=12V$, $\alpha = 0.29$, $I_L=7.5A$, $R_m=15.9\Omega$, $C_i=150F$, $L=1.5mH$ and $V_i=35V$.

This transfer function has two complex conjugate poles at $S=1.0e+002 * (-2.0889 \pm 5.7458i)$, the response for a step increase in duty ratio is illustrated in Fig (7).

The signal has a negative steady-state gain of about 169.5, the rise time is about 2 ms, the settling time is about 14 ms, the peak overshoot is about 34.2%, the natural frequency is 611 rad/S, and the damping factor is 0.34.

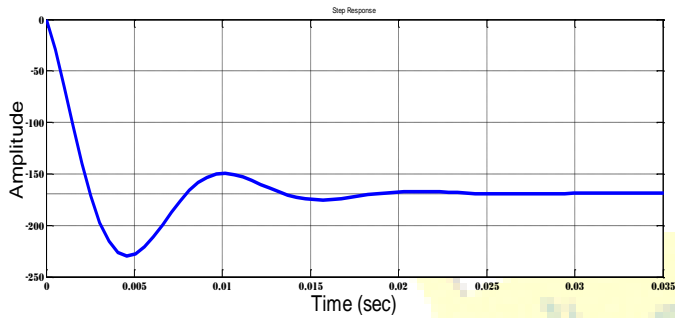


Fig.7 Array voltage response to a step increase in duty ratio.

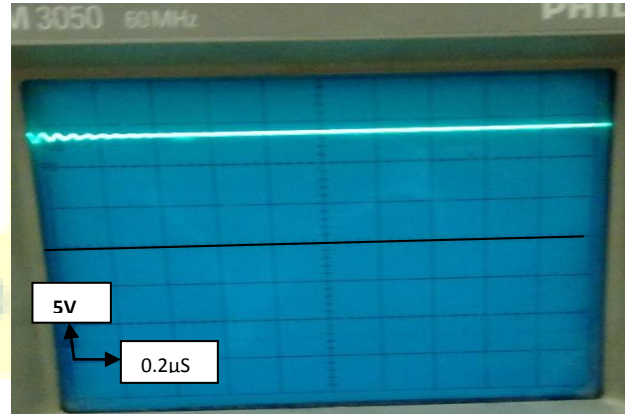


Fig (9-a) Battery voltage for 17V input voltage

7. Experimental results

The complete system has been designed and implemented in the laboratory, using variable power supply instead of the SPV panel based on software package. The battery charger has been tested for 12V lead acid battery, figure (8) shows the implemented prototype converter with 12V lead acid battery. And the figures (5.10A-5.10B),(5.11A-5.11B) show battery voltage and charging current respectively for 17V and 10V input voltage

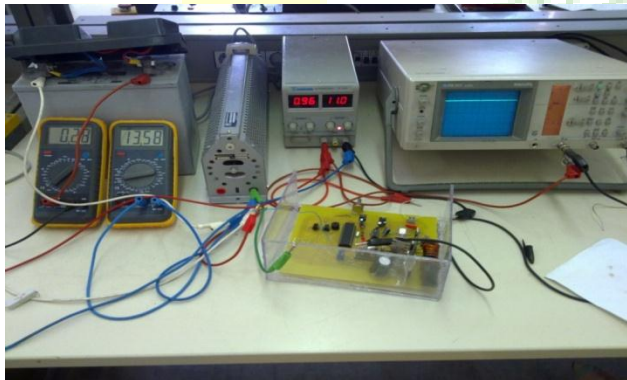
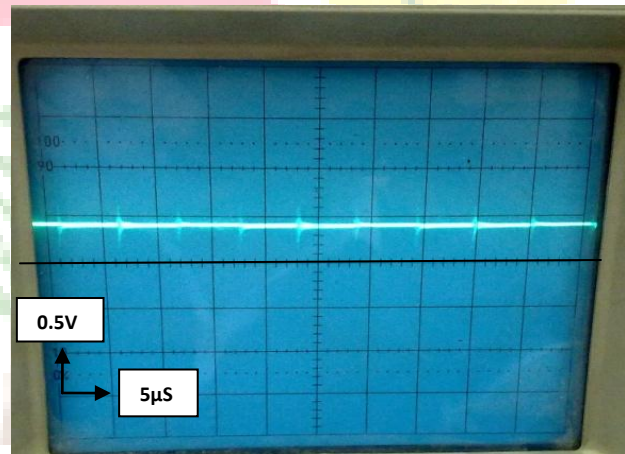


Fig.8 Implemented prototype converter with 12V lead acid battery.



Fig(9-b) Charging current for 17V input voltage



Le 3^{ème} Séminaire International sur les Energies Nouvelles et Renouvelables

The 3rd International Seminar on New and Renewable Energies

Unité de Recherche Appliquée en Energies Renouvelables,

Ghardaïa – Algérie 13 et 14 Octobre 2014

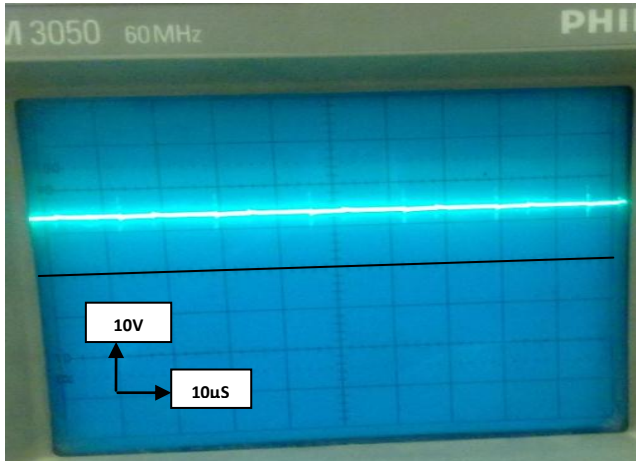


8- Conclusion

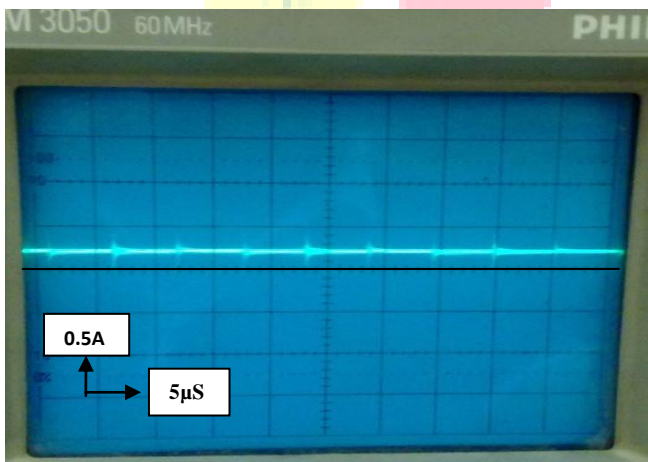
This paper concerns with analyze, design, and realization of DC/DC buck-boost converter to operate in PV system. this converter can be used as a buck converter or as a boost converter or as a buck-boost converter by selecting different combinations of the switches .The complete system has been designed and implemented in the laboratory, using a variable power supply instead of the SPV panel based on software package. The experimental results of the implemented prototype circuit confirm the integrity of the proposed circuit. This converter can be use in various applications like solar battery charger, mobile charger and for DC power supplies .

9. References

- [1] Robert S. Weissbach and Kevin M. Torres, "A non inverting buck-boost converter with reduced components using a microcontroller", *IEEE Journal* 10.1109/SECON. April2001.
- [2] M Hasaneen , Adel A. Elbaset Mohammed " DESIGN AND SIMULATION OF DC/DC BOOST CONVERTER" B. Faculty of Eng., Al-Azhar University, Kena, Egypt, *IEEE Journal*, 1933,03 ,2008 , page03.
- [3] M.Boukli Hacene Omar "Conception et Réalisation d'un générateur photovoltaïque muni d'un convertisseur MPPT pour une meilleure gestion énergétique", magister thesis, University of Tlemcen, decembre 2011.
- [4] "How to Design an Efficient DC-DC Converter Using the DS1875 PWM Controller" APPLICATION NOTE 4332, oct 18 2012.
- [5] Adriana Trejos & Daniel Gonzalez & Carlos Andres Ramos. "Modeling of Step-up Grid-Connected Photovoltaic Systems for Control Purposes" " journal/energies,2012" page 14.
- [6] Shen Guo" The Application of Genetic Algorithms to Parameter Estimation in Lead-Acid Battery Equivalent Circuit Models", bachelor dissertation University of Birmingham, may 2010, page 40.
- [7] MARIAN K. KAZIMIERCZUK "Pulse-width Modulated DC-DC Power Converters" A John Wiley and Sons, Ltd, Publication, Wright State University Dayton, Ohio, USA,2008 ,page56.



Fig(10-a) Battery voltage for 10V input voltage



Fig(9-b) Charging current for 17V input voltage

As we have seen in the last figures at various input voltage, output charging voltage remains about constant. This is mainly constant voltage charging of the battery ,as the input voltage increase the charging current will increasing too, decreasing the time of battery charging. The charging current and load or the load is different due to variable internal resistance of the battery because it depends on the temperature during charging.